Cryogenics 123 (2022) 103452

Contents lists available at ScienceDirect

Cryogenics

journal homepage: www.elsevier.com/locate/cryogenics

Investigations on a 1 K hybrid cryocooler composed of a four-stage Stirling-type pulse tube cryocooler and a Joule-Thomson cooler. Part B: Experimental verifications

Haizheng Dang [a,b,c,d,*], Tao Zhang [a,c], Bangjian Zhao [a,c], Yongjiang Zhao [a,c], Jun Tan [a], Han Tan [a,c], Renjun Xue [a,c], Shiguang Wu [a,c], Yujia Zhai [a,c]

[a] State Key Laboratory of Infrared Physics, Shanghai Institute of Technical Physics, Chinese Academy of Sciences, 500 Yutian Road, Shanghai 200083, China
[b] Shanghai Research Center for Quantum Sciences, Shanghai 201315, China
[c] University of Chinese Academy of Sciences, Beijing 100049, China
[d] Shanghai Boreas Cryogenics Co., Ltd, Shanghai 201802, China

ARTICLE INFO

Keywords:
1 K hybrid cryocooler
Four-stage Stirling-type pulse tube cryocooler
Joule-Thomson cooler
Experimental verifications

ABSTRACT

In this part, a hybrid cryocooler composed of a four-stage Stirling-type pulse tube cryocooler (SPTC) and a Joule-Thomson cryocooler (JTC) is worked out to verify the theoretical analyses carried out in Part A. The heat loss on each precooling stage is calculated to evaluate the feasibility of thermal coupling between the SPTC and the JTC. The JT compressors are tested and then the compression capacity is studied. A bypass-accelerated-cooling approach is adopted to speed up the cool-down process. The experimental results show that with He-4 in the SPTC and He-3 in the JTC, a no-load temperature of 1.36 K is reached when the three precooling temperatures are kept at 71.2 K, 40.5 K and 8.12 K, respectively. The cooling capacity of 13.9 mW at 1.8 K is measured with the JT loop high pressure and the last stage precooling temperature being at 0.5 MPa and 8.1 K, respectively. Satisfactory agreements are observed between theoretical and experimental studies.

1. Introduction

In Part A [1], a hybrid cryocooler composed of a four-stage Stirling-type pulse tube cryocooler (SPTC) and a Joule-Thomson cryocooler (JTC) which aims at reaching a temperature of 1.0 K has been theoretically analyzed, in which the structural design is described in detail, and the enthalpy flow and mass flow rate models are developed and then combined to study the cooling performance of the hybrid cryocooler. The theoretical studies investigate the working mechanisms in the JTC and then suggest the systematic optimization on the hybrid cryocooler. In this part, the experimental verifications of the developed hybrid cryocooler will be presented, and then the theoretical and experimental results will be compared and discussed.

2. Experimental verifications

2.1. Experimental setups

The geometric details of the developed 1 K hybrid cryocooler can be found in Fig. 1 in Part A [1].

In this part, we focus on the actual 1 K cold head, as shown in Fig. 1, and Fig. 2 shows the cold heads coupled to the corresponding compressors together with the experimental apparatus. The cold head of the JTC is thermally coupled with that of the four-stage SPTC. The four-stage SPTC is driven by two linear compressors [2,3], in which the first two cold fingers are driven by one and the last two fingers by the other one. The JTC is driven by the JT compressor unit composed of four linear compressors, which provides unidirectional flow for the JT cycle with the high pressure P_U and the low pressure P_D, respectively.

Two radiation shields are mounted on the first and fourth stage cold heads of the SPTC, to provide the JTC with cold backgrounds at around 70 K and 8 K, respectively. The shields are made of the copper slices and plated with highly reflective materials on the surfaces to minimize the

* Corresponding author at: State Key Laboratory of Infrared Physics, Shanghai Institute of Technical Physics, Chinese Academy of Sciences, 500 Yutian Road, Shanghai 200083, China.
E-mail address: haizheng.dang@mail.sitp.ac.cn (H. Dang).

https://doi.org/10.1016/j.cryogenics.2022.103452
Received 23 July 2021; Received in revised form 26 October 2021; Accepted 15 March 2022
Available online 18 March 2022

Nomenclature

A	area (m^2)
AC	alternating current
BAC	bypass-accelerated-cooling
CHEX	counterflow heat exchanger
DC	direct current
l	length (m)
$\dot{m}$	mass flow rate (mg s^{-1})
P	pressure (Pa)
PHEX	precooling heat exchanger
T_C	cooling temperature (K)
T_H	ambient temperature (K)
T_{pre}	precooling temperature (K)
U	output voltage

Greeks

ε	emissivity
σ	Stefan-Boltzmann constant (5.67×10^{-8} W m^{-2} K^{-4})
λ	thermal conductivity (W m^{-1} K^{-1})

Subscripts

D	downstream, low pressure of JT cycle
U	upstream, high pressure of JT cycle

Superscripts

RS	radiation heat loss of radiation shield
CC	conduction heat loss of CHEX
RC	radiation heat loss of CHEX

radiation heat loss.

As shown in Fig. 1, the three precooling heat exchangers (PHEXs) of the JTC are made of oxygen-free copper filled with porous media to enhance its heat exchange capacity. The first and third PHEXs are mounted on the base plates of the two radiation shields, respectively, while the second one is directly coupled with the second cold head of the SPTC. The counter-flow heat exchanger (CHEX) is made of several concentric stainless-steel tubes, with the high-pressure tube being inside while the low-pressure tube outside. The four-stage CHEXs are all wound into spiral shapes and then connected by the three PHEXs. The evaporator, with an orifice inside, is located at the end of the fourth stage CHEX and connected to the bypass line. The cooling powers will be provided by the evaporator.

As shown in Fig. 2, six AC power sources are used to supply the input powers, in which two ones are for the SPTC compressors while the other four ones for the JT compressors. Each power source can independently provide the adjustable voltage, current and frequency. Two pressure sensors are set at the inlet and outlet of the JT compressor unit to measure the high and low pressures of the cycle, respectively. A mass flowmeter (MFM) is placed in the JT loop to monitor the mass flow of He-3. Several Cernox CX-1050X temperature sensors are used to measure the temperatures at PHEXs, evaporator and points before throttling.

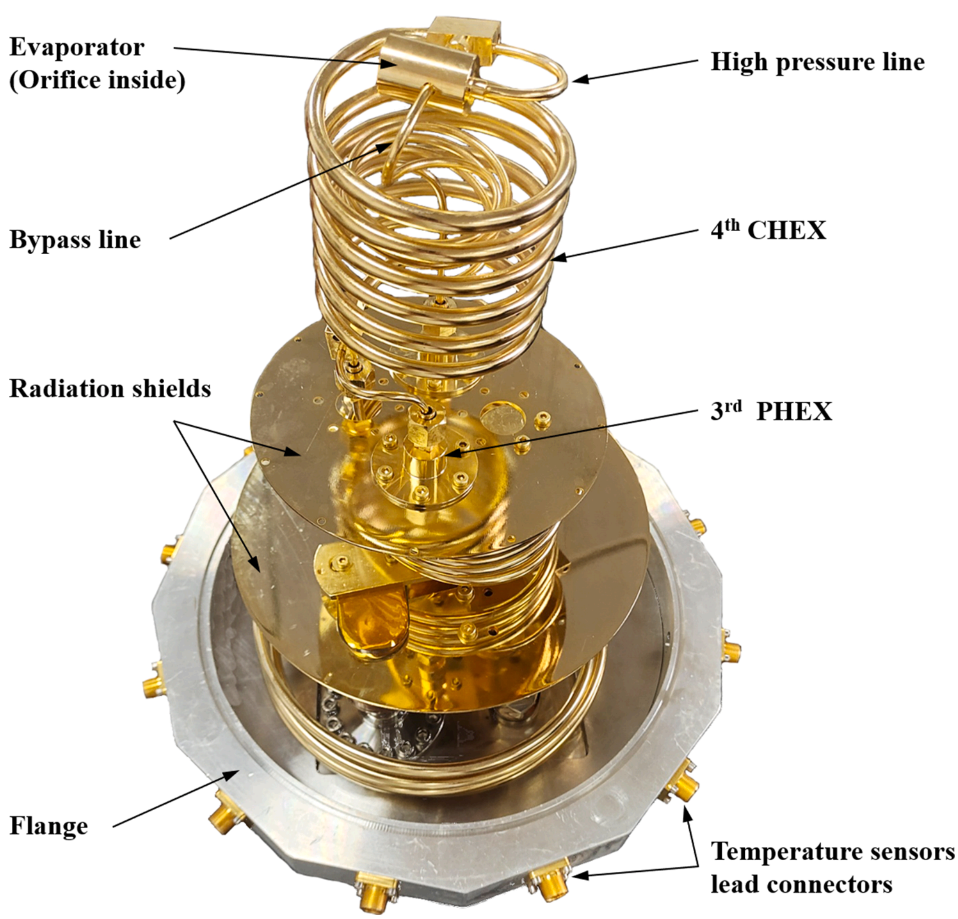

Fig. 1. Photo of the actual hybrid cryocooler cold head.

A heating resistor is employed to impose the required heat load on the evaporator to evaluate the cooling capacity. All experimental data are collected by a data acquisition.

2.2. Heat loss calculation

The purpose of heat loss estimation is to ensure that the performance of the four-stage SPTC, as a precooling cooler, can meet the working requirements of the JTC cycle. According to Ref. [3], with He-4 used as the working fluid, the cooling powers at the four stages of the four-stage SPTC are 4.4 W at 70 K, 1.0 W at 40 K, 0.1 W at 15 K, and 0.08 W at 8 K, respectively.

The heat loss of the hybrid cryocooler consists of two parts, in which one is the radiation heat loss of the two radiation shields and the CHEXs, and the other is the axial conduction heat loss of the CHEXs at different temperature ranges. The dimensional parameters of the two radiation shields and four-stage CHEXs are shown in Table 1 and Table 2, respectively.

The radiation heat losses of the two radiation shields are calculated by the following equations:.

$$\Delta {Q_1}^{RS} = A_1 \varepsilon \sigma \left(T_H^4 - T_{pre1}^4\right) \tag{1}$$

$$\Delta {Q_2}^{RS} = A_2 \varepsilon \sigma \left(T_{pre1}^4 - T_{pre3}^4\right) \tag{2}$$

where A is the radiation shield area, ε is the surface emissivity, σ is the Stefan-Boltzmann constant, and $T_H = 300$ K, $T_{pre1} = 70$ K, $T_{pre3} = 8$ K.

The conduction heat loss and the radiation heat loss of the 1st stage CHEX can be regarded as the heat loads on the 70 K stage, which are calculated as follows:.

$$\Delta {Q_1}^{CC} = \frac{\pi}{4 l_1} \left[\left({D_{o1}}^2 - {D_{i1}}^2\right) + \left({d_{o1}}^2 - {d_{i1}}^2\right) \right] \int_{70}^{300} \lambda(T)\, dT \tag{3}$$

$$\Delta {Q_1}^{RC} = \pi D_{o1} \varepsilon \sigma \int_0^{l_1} \left[300^4 - T_1(x)^4\right] dx \tag{4}$$

where l_1 is the length of the 1st CHEX, λ(T) is the thermal conductivity of stainless steel as a function of temperature, T_1(x) is the temperature change of the 1st CHEX along the axial direction. The above two equations are also applicable to the other three CHEXs.

The calculated heat loss on the cold heads of the SPTC and JTC are summarized in Table 3. It is observed that the total heat loss on each cold head is within its corresponding cooling capacity, which indicates that all the PHEXs of the JTC could reach the expected temperatures. Besides,

Table 1
Dimensional parameters of the two radiation shields.

Stage	Temperature (K)	Diameter (mm)	Height (mm)	Emissivity
1st	70	180	300	0.03
2nd	8	110	180	0.03

Table 2
Dimensional parameters of the CHEXs.

Stage	Temperature range	Length (m)	D_o (mm)	D_i (mm)	d_o (mm)	d_i (mm)
1st	300 K to 70 K	2.2	7	6.5	4.2	3.6
2nd	70 K to 40 K	1.0	6.5	6	4	3.4
3rd	40 K to 8 K	1.3	6	5.5	3.6	3
4th	8 K to 1 K	1.8	5	4.5	2.8	2.2

where D_o and D_i stand for the outer and inner diameter of the low pressure tube, respectively, and d_o and d_i stand for the outer and inner diameter of the high pressure tube, respectively.

Table 3
Calculated heat loss on the four cold heads of the SPTC.

Stage	ΔQ^{RS}	ΔQ^{CC}	ΔQ^{RC}	Total heat loss (W)	Cooling capacity (W)
70 K	3.03 W	10.8 mW	284.3 mW	3.325	4.4
40 K	—	1.57 mW	0.47 mW	0.002	1.0
15 K	—	—	—	—	0.1
8 K	3.32 mW	0.56 mW	0.97 mW	0.005	0.08
1 K	—	0.01 mW	10^{-4} mW	10^{-5}	—

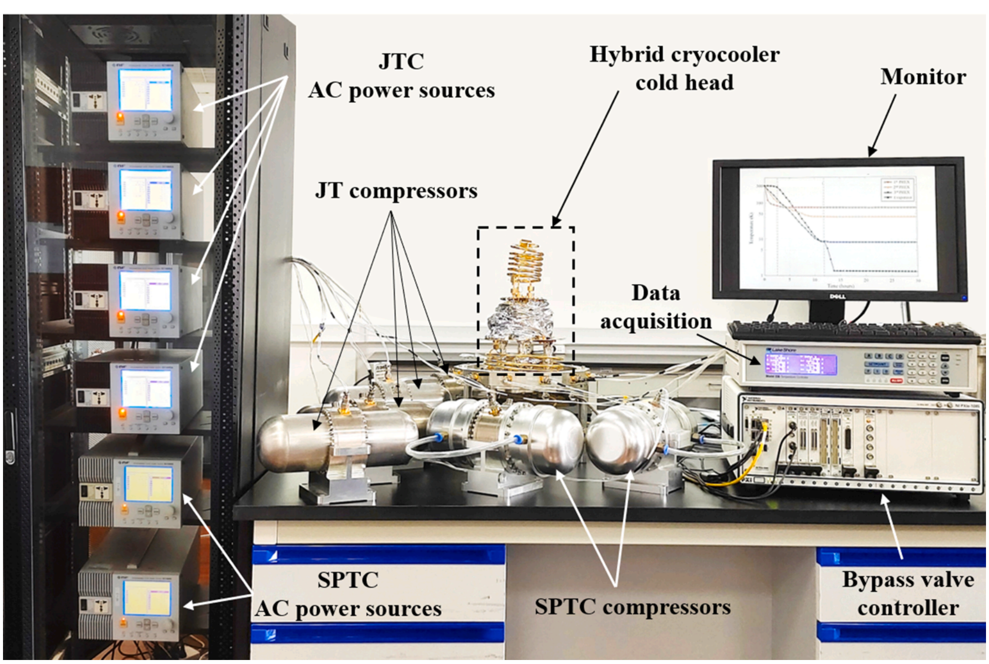

Fig. 2. Hybrid cryocooler cold heads coupled to corresponding compressors together with experimental apparatus.

the calculated heat loss on the evaporator is only around 0.01 mW, which is negligible compared to the cooling capacity that will be tested in the following sections.

2.3. JT compressor unit

The JT compressor unit consists of the four linear JT compressors, which is studied separately at room temperature to evaluate its extreme suction (low) pressure and compression performance. The adjustable needle valves are adopted to connect the inlets and outlets of the four linear compressors one by one, thereby forming a closed loop. The design frequencies from the first to the fourth compressor are 30 Hz, 40 Hz, 40 Hz and 80 Hz, respectively.

Fig. 3 shows the effect of the charge pressure on P_D, P_U and the total pressure ratio of the JT compressor unit in two mass flow rate cases. In Case 1, the needle valve is completely closed, and thus the mass flow rate is zero. When the charge pressure is 50 kPa, the lowest suction pressure can reach 3 kPa, which corresponds to a discharge pressure of 330 kPa and a compression ratio of 110. When the charge pressure increases, both the suction and discharge pressure increase while the total pressure ratio gradually decreases. For instance, as the charge pressure increasing from 50 kPa to 190 kPa, the pressure ratio decreases from 110 to 80.

In Case 2, the needle valve is fixed to keep the mass flow rate at 2 mg/s. It is observed that the variations of P_D, P_U and the pressure ratio with the charge pressure are similar to those in Case 1. However, due to the effect of the mass flow rate, P_D in Case 2 is higher than that in Case 1, while P_U in Case 2 is lower than that in Case 1. Besides, compared with Case 1, the pressure ratio in Case 2 decreases more drastically with the increasing charge pressure. When the charge pressure is 190 kPa, P_D increases from 7 kPa to 12 kPa, P_U declines from 840 kPa to 624 kPa, and the corresponding pressure ratio reduces from 80 to 52.

In summary, the increase of the charge pressure is always adverse to the compressor unit to obtain a lower suction pressure, but to a certain extent, it raises the upper limit of the discharge pressure, even though the overall pressure ratio is decreased. On the other hand, the mass flow is detrimental to the compressor to achieve a higher compression ratio. Given that the mass flow is inevitabe when the JTC works and there is always an actual pipe pressure drop in the JTC, the expected P_D after throttling will be higher than the suction pressure tested at room temperature, and the corresponding pressure ratio will be even smaller.

2.4. Cool-down process

Fig. 4 shows the cool-down curve of the hybrid cryocooler with no load. This process can be divided into three stages according to the opening and closing of the bypass valve, which is an electrically controlled adjustable needle valve located at the inlet of the last stage bypass line. The three stages are as follows:.

(i) Stage 1 (0 to 2.5 h): The four-stage SPTC starts to work, but neither the JTC nor the bypass valve is turned on, so that the temperatures of PHXEs (T_{pre1}, T_{pre2} and T_{pre3}) drop as soon as possible. It is observed that the evaporator temperature in this stage decreas very slow, for which the reason is that the evaporator can only exchange heat with the 3rd PHEX through the heat conduction, and the cross-sectional area of the CHEX tube is very small.

(ii) Stage 2 (2.5 to 11.5 h): When T_{pre1} reaches around 80 K, the JTC starts to work and the bypass valve is turned on. The fluid in the JT loop begins to circulate, making the temperature of the evaporator drop by heat convection. In order to speed up this process, a bypass-accelerated-cooling (BAC) approach is proposed. The details are as follows:.

First, through a series of tests, the optimal mass flow rate changing with T_{pre3} in the fastest cooling speed is determined.

Second, the variation of the mass flow rate is inversely proportional to that of the input voltage (U) of the bypass valve which is controled by an DC power, thereby a direct functional relationship between T_{pre3} and the DC power output voltage can be established and then this function can be input to the controller.

Third, in the cool-down process, the collected T_{pre3} is analyzed by the controller and the output voltage of the DC power is adjusted according to the above functional relationship, by which the automatic adjustment of the bypass valve is realized to achieve the fastest cooling goal. The feedback control principle is shown in Fig. 5.

(iii) Stage 3 (11.5 to 30 h): When the temperatures of the evaporator and the 3rd PHEX are very close, the bypass valve is then completely closed. The working fluid passes through the orifice with a diameter of 20 μm to produce the throttling effect. It is noted that the evaporator temperature drops very fast and then achieves the lowest cooling temperature (T_C) of 1.36 K after about 2 h. Meanwhile, the three T_{pre} also reach their corresponding minimum temperatures 71.2 K, 40.5 K, and 8.12 K, respectively, which are very close to the values calculated in Section 2.2. The cooling temperature is continuously monitored for about 16 h, as shown in Fig. 6, and the fluctuations of less than ± 5 mK are observed during this period. The total power consumption of the SPTC compressors is 320 W while the input powers of the four JT compressors from the first to the fourth stage are 6 W, 8 W, 12 W and 20 W, respectively.

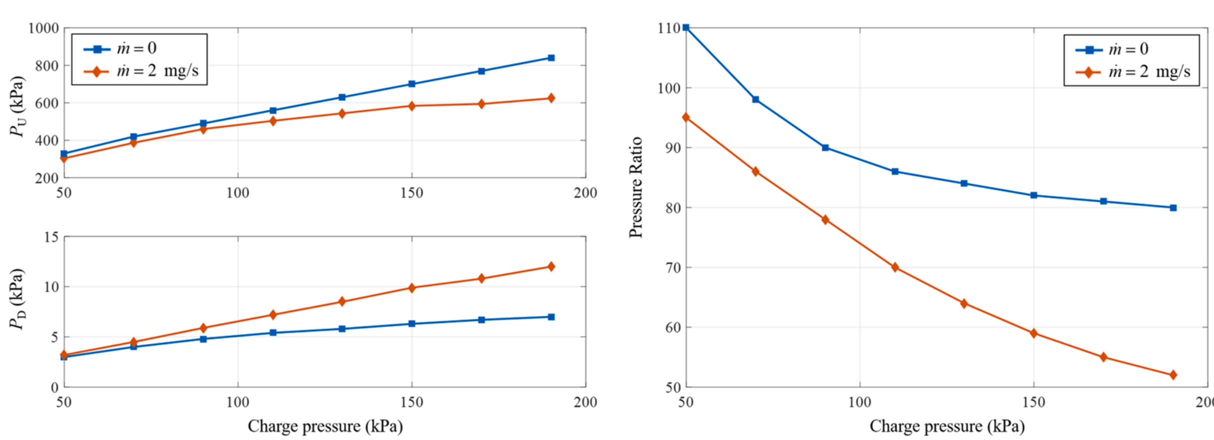

(a) (b)

Fig. 3. Effect of charge pressure on (a) P_D, P_U and (b) pressure ratio in two mass flow rate cases.

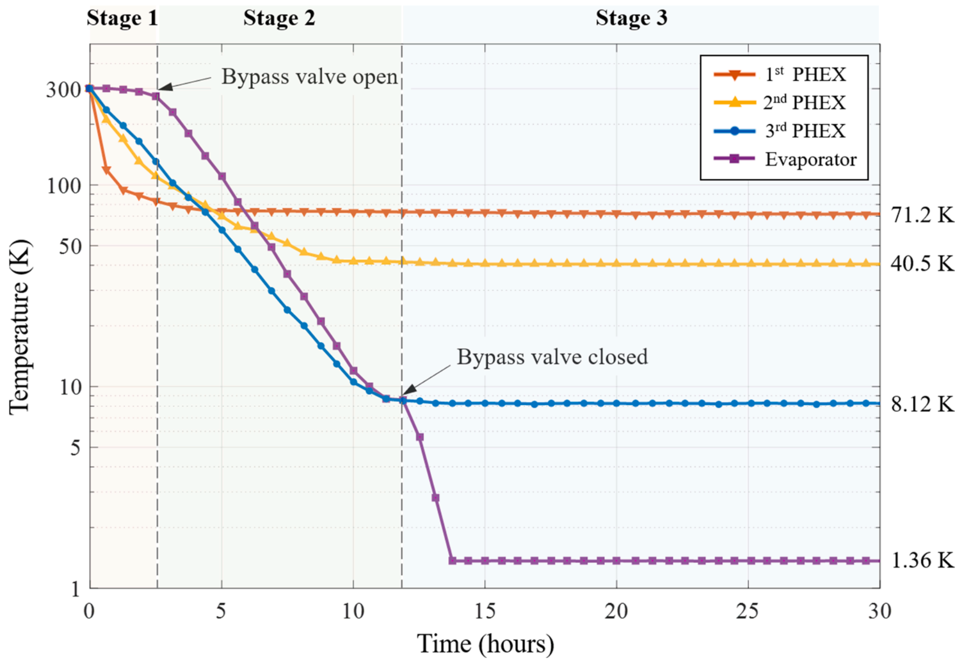

Fig. 4. Cool-down process of the hybrid cryocooler by using the BAC approach.

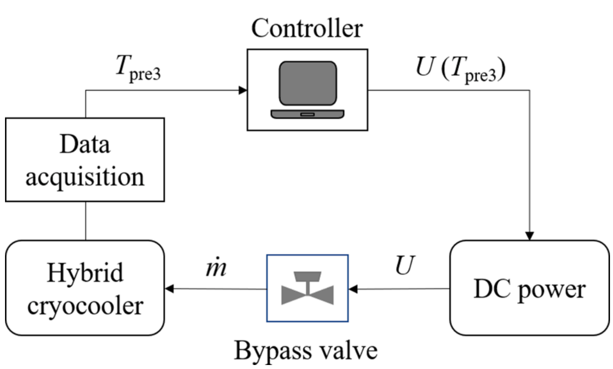

Fig. 5. Feedback control principle of the BAC approach.

Fig. 7 shows the variation of P_U, P_D and mass flow rate during stage 2 cooling process in the fastest cooling mode. It is observed that T_{pre3} gradually decreases and the mass flow rate also reduces from 10 mg/s to 0.92 mg/s. When the bypass valve is completely closed, the remaining value is only the mass flow rate through the orifice. In this process, as the opening of the bypass valve decreases, in the JT loop the high pressure P_U becomes higher while the low pressure P_D does lower. Finally, when the bypass valve is truned off, both P_U and P_D keep unchanged and then the throttling process begins. When the evaporator temperature reaches the lowest value of 1.36 K, the measured P_D is 3.2 kPa. By comparisions, the saturated vapor pressure of He-3 at 1.36 K is 4.5 kPa, which indicates that there exists a pressure drop of about 1.3 kPa in the low-pressure pipeline.

2.5. Cooling performance characteristics

In section 2.3, the compression capacity of the JT compressor unit without the mass flow rate has been tested. To further verify the theoretical analyses conducted in Part A [1], P_D needs to be stabilized at a relatively high value so that P_U can be changed by adjusting the input power of the JT compressor unit to obtain data under different operating conditions. Therefore, with a charge pressure of 0.19 MPa and P_D kept at 12 kPa, a heat load is applied to the evaporator to evaluate the cooling capacity of the hybrid cryocooler.

Fig. 8 shows the variations of the mass flow rate with P_U at $T_C = 1.8$ K and $T_{pre3} = 8.1$ K. The theoretical values are recalculated under the cooling temperature of 1.8 K based on the mass flow rate model presented in Part A [1]. The experimental results show that as P_U increases from 0.2 MPa to 0.6 MPa, the mass flow rate correspondingly increases from 1.6 mg/s to 2.8 mg/s. Although the measured values are slightly smaller than the calculated ones, the changing trends of the two are consistent, which verifys that the theoretical analyses.

Fig. 9 presents the variations of the cooling capacity with P_U under different T_{pre3}, in which the theoretical values are also obtained according to the gross cooling capacity model that combines the enthalpy flow and mass flow rate models in Part A [1]. Given that $T_{pre3} = 8.1$ K, as P_U increases from 0.2 MPa to 0.45 MPa, both of the theoretical and experimantal cooling capacities first increase rapidly, then the rising trend slows down in the range of 0.45 MPa to 0.5 MPa. Both of them reach their highest points at 0.5 MPa, and then gradually decrease.

It should be noted that, in the actual experiments, when the cooling capacity was measured, on the evaporator at around 1 K a heating resistor must be installed. The heating resistor at around 1 K and the AC power source at room temperature are connected by two copper wires. When the heating resistor works, the lead wires will generate Joule heat, which increases with the measured cooling power. This factor was not considered in the model given in Part A. Therefore, the theoretical cooling capacity obtained by the model in Ref [1] should subtract the heat leakage caused by the Joule heat. Based on the above analyses, a 15.6 mW of the theoretical cooling capacity is obtained. In the experiments, the measured maximum cooling power is 13.9 mW. The discrepancy between simulation and experiment is acceptable.

Compared with the situation when $T_{pre3} = 8.1$ K, for $T_{pre3} = 10$ K and $T_{pre3} = 12$ K, the cooling capacity continue to increase with the increasing P_U, reaching 12 mW and 10.8 mW at $P_U = 0.6$ MPa, respectively. Although there are still differences between the measured values and the theoretical ones, the trends of the two are very similar. The above results verify that the conclusion in Part A [1] that the decrease of T_{pre3} is beneficial to enhance the cooling capacity and there is indeed an optimal P_U under the condition of $T_{pre3} = 8.1$ K to maximize the cooling capacity.

Table 4 gives the input power to the hybrid cryocooler and the

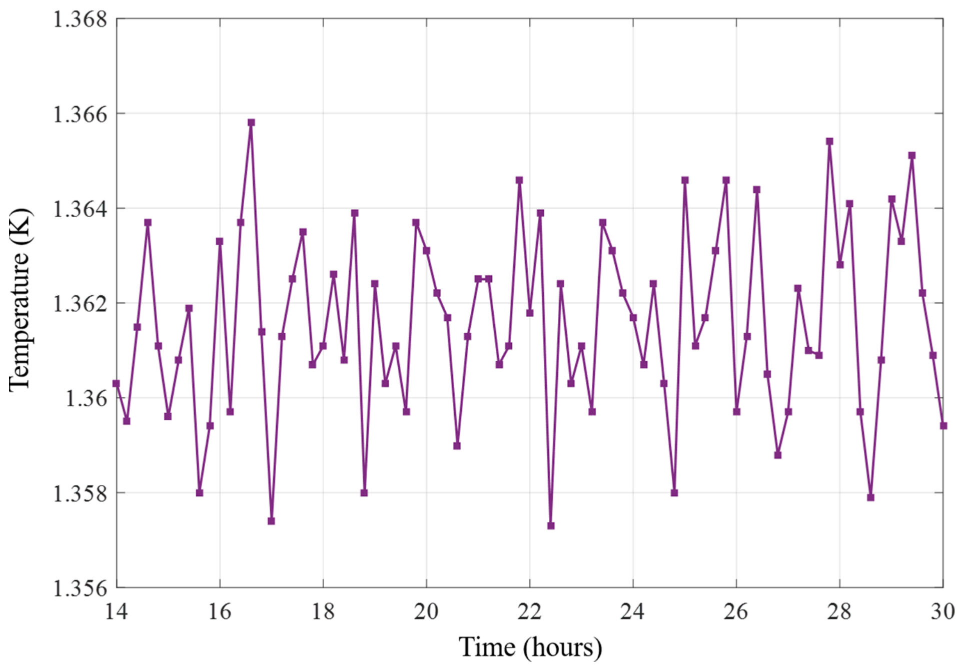

Fig. 6. Cooling temperature fluctuation curve.

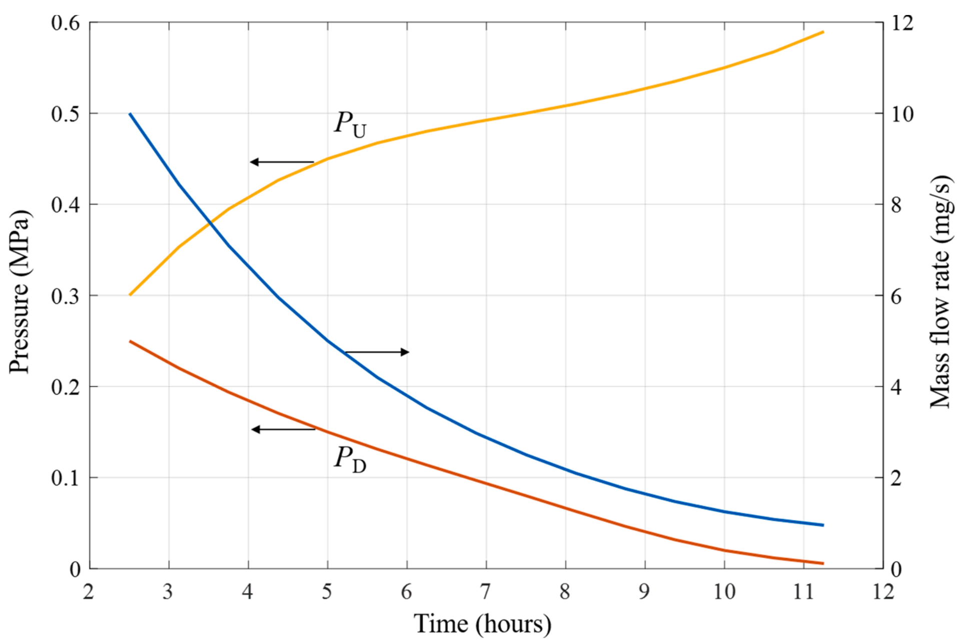

Fig. 7. Change of P_U, P_D and mass flow rate with time during stage 2 cooling process.

corresponding figure of merit (FOM) when the maximum cooling capacity is achieved under different T_{pre3}. Since the input power of the SPTC accounts for more than 85% of the total power consumption, when T_{pre3} increases from 8.1 K to 12 K, the input power of the SPTC decreases, thereby resulting in a decrease in the total input power of the hybrid cryocooler from 360 W to 345 W. However, due to the high cooling capacity at $T_{pre3} = 8.1$ K, the FOM under this condition, namely 0.64%, is higher than that at $T_{pre3} = 10$ K and $T_{pre3} = 12$ K, which is 0.56% and 0.52%, respectively. Compared with a three-stage pulse tube cryocooler precooling a JT cooler designed by Petach *et al* [4], which has a best predicted FOM of 0.38%, the optimal 0.64% FOM of this developed four-stage SPTC/JTC hybrid cryocooler is 1.68 times that of the former.

In summary, based on the experimental investigation, the developed hybrid cryocooler is capable of achieving a no-load temperature of 1.36 K and also providing a cooling power of 13.9 mW at 1.8 K. Satisfactory agreements are observed between theoretical and experimental studies.

3. Conclusions

This paper conducts the experimental verifications of a hybrid cryocooler composed of a four-stage SPTC and a JTC discussed in Part A [1]. The actual hybrid cryocooler is worked out and then the experimental results are compared with the theoretical ones.

The heat loss on each precooling stage is first calculated to evaluate the feasibility of thermal coupling between the SPTC and the JTC. And

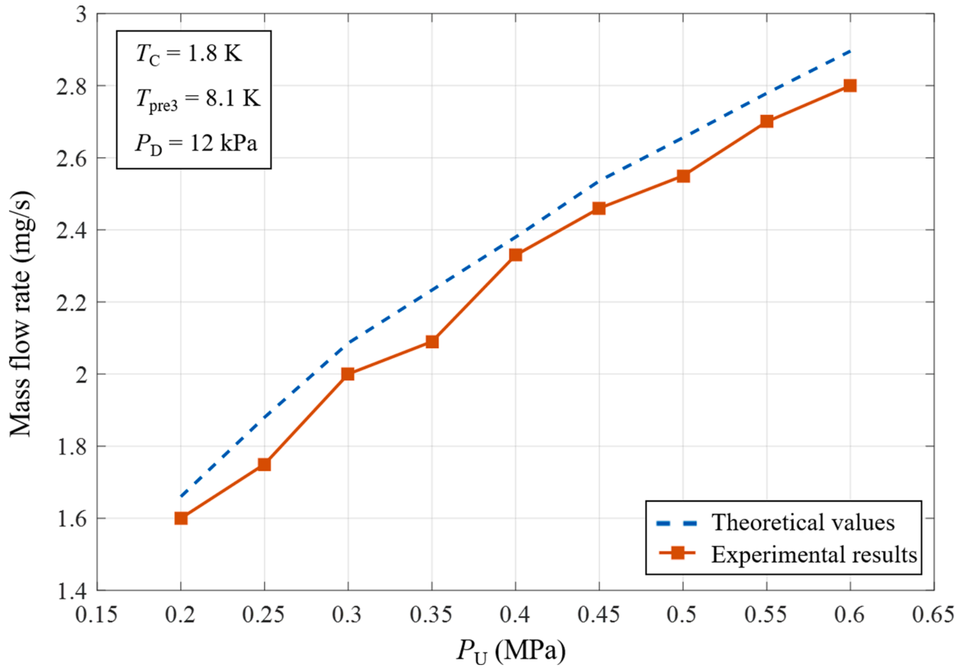

Fig. 8. Effect of P_U on mass flow rate at $T_C = 1.8$ K and $T_{pre3} = 8.1$ K.

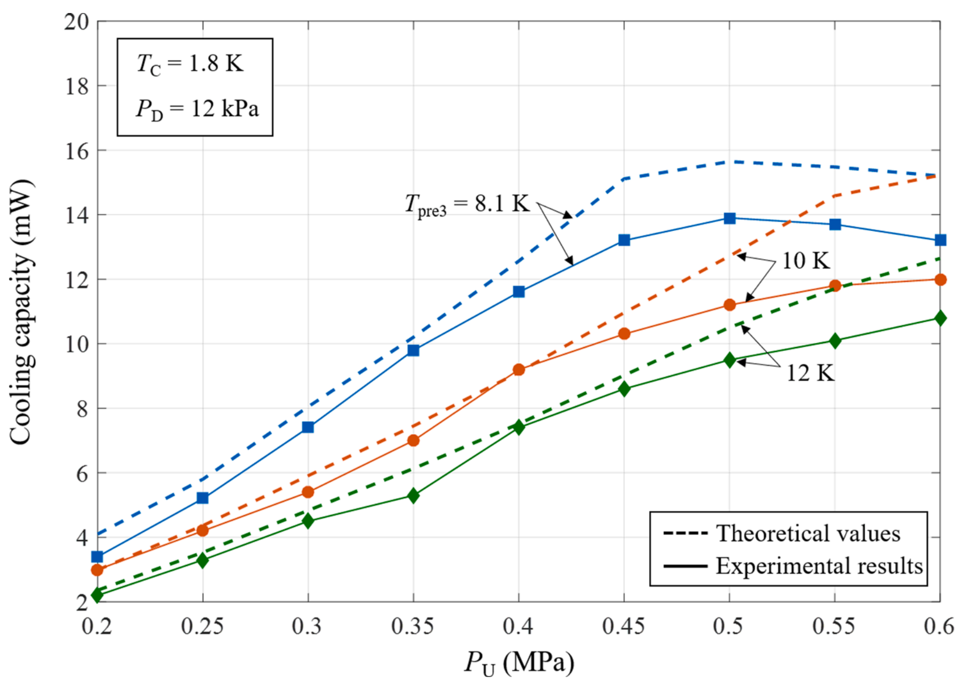

Fig. 9. Effects of P_U and T_{pre3} on cooling capacity.

Table 4
Input power and FOM of the hybrid cryocooler.

T_{pre3}	$Q_{C,max}$ (mW)	Input power to compressors (W)			FOM (%)
		SPTC	JT	Total	
8.1 K	13.9	320	40	360	0.64
10 K	12	310	42	352	0.56
12 K	10.8	300	45	345	0.52

then the JT compressor unit consisting of four linear compressors are tested in which the compression capacities with and without mass flow rate are studied, respectively. A bypass-accelerated-cooling approach is put forward and then applied to speed up the cool-down process. The experimental results show that with He-4 in the SPTC and He-3 in the JTC, a no-load temperature of 1.36 K is reached when the three pre-cooling temperatures are kept at 71.2 K, 40.5 K and 8.12 K, respectively. The cooling capacity of 13.9 mW at 1.8 K is measured when the JT loop high pressure is 0.5 MPa and the last stage precooling temperature is 8.1 K.

Satisfactory agreements are observed between theoretical and experimental studies. The experimental results also clearly indicate that the developed hybrid cryocooler has already possessed the capacity of providing the appropriate cooling for the actual superconducting nanowire single-photon detector (SNSPD), and thus suggest a promising prospect for its potential application in the next generation space quantum information technology.

CRediT authorship contribution statement

Haizheng Dang: Conceptualization, Methodology, Supervision, Investigation, Writing – original draft, Writing – review & editing. **Tao Zhang:** Methodology, Investigation, Data curation, Writing – original draft. **Bangjian Zhao:** Methodology, Investigation, Data curation. **Yongjiang Zhao:** Methodology, Investigation, Data curation. **Jun Tan:** Methodology, Investigation, Data curation. **Han Tan:** Investigation. **Renjun Xue:** Investigation. **Shiguang Wu:** Investigation. **Yujia Zhai:** Investigation.

Declaration of Competing Interest

The authors declare that they have no known competing financial interests or personal relationships that could have appeared to influence the work reported in this paper.

Acknowledgements

This work is supported by the National Natural Science Foundation of China (Grant No. 52076210) and Shanghai Municipal Science and Technology Major Project (Grant No. 2019SHZDZX01). It is also partly financially supported by Shanghai Municipality (Grant Nos. 18511110100, 19511106800, 2019-jmrh2-kj2 and 2021-cyxt2-kj09).

References

[1] Zhang T, Dang HZ. Investigations on a 1 K hybrid cryocooler composed of a four-stage Stirling-type pulse tube cryocooler and a Joule-Thomson cooler. Part A: Theoretical analyses and modeling. Cryogenics 2021;116:103282.

[2] Dang H. Development of high performance moving-coil linear compressors for space Stirling-type pulse tube cryocoolers. Cryogenics 2015;68:1–18.

[3] Dang HZ, Zha R, Tan J, et al. Investigations on a 3.3 K four-stage Stirling-type pulse tube cryocooler. Part B: Experimental verifications. Cryogenics 2020;105:103015.

[4] Petach M, Michaelian M, Nguyen T. Modifications to the MIRI cryocooler design to provide significant lift in the 2K to 4K range. IOP Conference Ser Mater Sci Eng 2020;755(1):012018. https://doi.org/10.1088/1757-899X/755/1/012018.